Frequency Pulling and Mixing of Relaxation Oscillations in Superconducting Nanowires

Emily Toomey,[1] Qing-Yuan Zhao,[1] Adam N. McCaughan,[1,2] and Karl K. Berggren[1,*]
[1]*Department of Electrical Engineering and Computer Science, Massachusetts Institute of Technology, Cambridge, Massachusetts 02139, USA*
[2]*National Institute of Standards and Technology, 325 Broadway, Boulder, Colorado 80305, USA*

(Received 28 September 2017; revised manuscript received 21 March 2018; published 14 June 2018)

Many superconducting technologies such as rapid single-flux quantum computing and superconducting quantum-interference devices rely on the modulation of nonlinear dynamics in Josephson junctions for functionality. More recently, however, superconducting devices have been developed based on the switching and thermal heating of nanowires for use in fields such as single-photon detection and digital logic. In this paper, we use resistive shunting to control the nonlinear heating of a superconducting nanowire and compare the resulting dynamics to those observed in Josephson junctions. We show that interaction of the hotspot-impedance with an external shunt produces high-frequency relaxation oscillations with similar behavior to that observed in Josephson junctions due to their ability to be modulated by a weak periodic signal. In particular, we use a microwave drive to pull and mix the oscillation frequency, resulting in phase-locked features that resemble the Shapiro steps observed in the ac Josephson effect. Microwave nanowire devices based on these conclusions have promising applications in fields such as parametric amplification and frequency mixing.

DOI: 10.1103/PhysRevApplied.9.064021

I. INTRODUCTION

Relaxation oscillators have been used to model a wide variety of nonlinear behavior found in biological and physical systems; for instance, cardiac rhythms [1] and modulated semiconductor lasers [2] have both been described by relaxation oscillation dynamics. While in the most basic sense, relaxation oscillations are comprised of a nonlinear element and a feedback cycle, it was observed early on that another property unique to relaxation systems is that their oscillation frequencies may be altered by the application of a weak periodic drive [1,3]. As a result, both the relaxation process and its response to external stimuli are vital to the characterization of a complete system.

Superconductors represent an ideal platform for studying and manipulating these types of oscillatory phenomena. In addition to having rapid nonlinear switching dynamics, their response changes with the temperature, current density, and the application of magnetic fields. This tunability allows for the effects of external drives to be observed. Perhaps one of the strongest manifestations of these oscillations in superconductors is the ac Josephson effect in which locking between a periodic drive and a Josephson junction's sinusoidal current-phase relationship produces zero-slope regions known as Shapiro steps in the current-voltage curve at intervals of $V_n = nhf/2e$, where f is the driving frequency, h is Planck's constant, e is the electronic charge, and n is the integer order of the step [4,5]. This relationship between frequency and voltage has been exploited in technologies such as the Josephson voltage standard [6,7] and superconducting analog-to-digital converters in which a Josephson junction produces single-flux quantum pulses at a frequency corresponding to the applied voltage [8]. Another form of a superconducting weak link known as the Dayem bridge proved to have similar ac behavior, with additional steps appearing at subharmonic values of the Shapiro voltage due to the Dayem bridge's multivalued periodic current-phase relationship [9–11]. Work by Calander *et al.* demonstrated that subharmonics can also occur in inductively shunted tunnel junctions by injection locking of relaxation oscillations; as the strength of the locking signal increased, the oscillation frequency was pulled toward the drive frequency, and mixing products were observed [12].

Unlike the tunneling of Josephson junctions, superconducting nanowires are governed by thermal transitions into the normal state as a result of Joule heating. Despite the lack of a sinusoidal current-phase relationship, they can support relaxation oscillations due to the nonlinear interactions between the resistive hotspot and the impedance of the external readout circuit, as previously demonstrated in superconducting nanowire single-photon detectors (SNSPDs) [13–15].

In work by Hadfield *et al.* [16], oscillations in high-inductance nanowires were attributed to the relaxation of a resistive hotspot through an inductor and resistive shunt.

*Corresponding author.
berggren@mit.edu

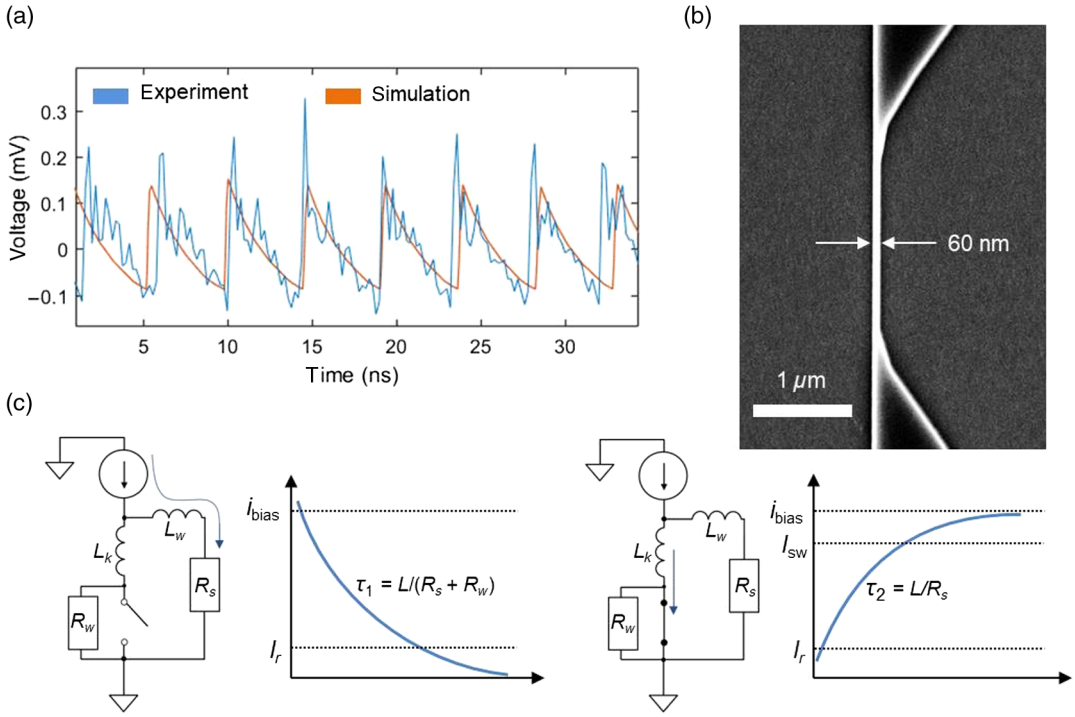

FIG. 1. (a) rf voltage output of the shunted nanowire ($R_s = 10\ \Omega$) when a bias-current ramp is applied. The blue trace corresponds to experimental data, and the red trace is the output of electrothermal simulations. (b) Scanning electron micrograph of the tapered nanowire. (c) Illustration of a basic relaxation model. The bias current is first diverted to the shunt after the nanowire switches to the normal state and then returns to the nanowire once superconductivity is restored. The total inductance L is the sum of the nanowire's kinetic inductance L_k and the inductance of the wire bond connections L_w. In our experimental setup, L_w dominates the total inductance.

The appearance of characteristics similar to those of Shapiro steps upon microwave radiation was suspected to be the result of phase locking of these relaxation oscillations to the external drive. There are three outstanding problems with the study in Ref. [16] that have since remained unresolved: (1) The dependence of the oscillation frequency on circuit parameters was not studied, (2) the voltage interval of the observed steps was not explained, and (3) no mechanism for the suspected locking behavior was presented. As such, while the similarity to the ac Josephson effect was observed, it was not fully characterized experimentally or analytically. A complete study of this phenomenon is, therefore, needed for the control and engineering of nanowire-based devices that take advantage of this effect.

Previous studies of these oscillations were done using typical SNSPDs of large kinetic inductance ($L_k =$ 200–500 nH) and an external load placed far from the local hotspot [14,16]. This setup limits the minimum time constants that can be observed, and, thus, the reported oscillation frequencies were often less than 200 MHz. To investigate fast oscillations of this nature while removing parasitic parameters from cabling, we present a study of the nonlinear dynamics in a short nanowire of <10-nH kinetic inductance and a shunt resistor mounted close to the chip, as summarized in Fig. 1. The experimental rf voltage output reveals distinct oscillations which are in agreement with both electrothermal simulations and a simple analytical model based on hotspot-relaxation. In this paper, we describe the influence of bias current and series inductance on these oscillations and study their time-averaged characteristics. By using microwave radiation, we demonstrate that the hotspot-oscillations can mix with a weak external signal and be pulled toward its frequency until becoming locked, thus providing a mechanism for the observed similarity to the ac Josephson effect. We emphasize that we do not expect these devices to act as Josephson junctions; rather, in this work, we show that they produce behavior that looks deceptively like a junction because of locking between their thermal oscillations and an external periodic drive.

II. METHODS

The nanowires studied in this paper are fabricated from a thick (approximately 40 nm) niobium nitride film deposited on Si substrates following the procedure described in Ref. [17]. Contact pads are defined by photolithography on evaporated Au and Ti. Superconducting nanowires are designed with tapers from 1 μm to a minimum width of 60 nm to minimize current crowding [18] and are written using electron-beam lithography (125 kV, Elionix) of hydrogen silsesquioxane resist, followed by development in 25% tetramethylammonium hydroxide and reactive ion etching in CF_4. The total length of the device

[see Fig. 1(b)] is 30 μm, with a 60-nm-wide center region about 1.5 μm long.

In order to shunt the nanowire, an external resistor of 10 Ω is placed in parallel less than 5 mm away on the printed circuit board (PCB). Aluminum wire bonds are used to make electrical connections to the contact pads and the shunt. All measurements are conducted in liquid helium at a temperature of 4.2 K, well below the critical temperature of the superconducting film ($T_c \sim 10.5$ K). Electrical transport characterization for current-voltage measurements is achieved using a four-point scheme and a sinusoidal current bias at a sweeping frequency of 10–20 Hz. dc output voltages are sent through a low-noise preamplifier (SRS560) before being read out by an oscilloscope. Microwave modulation is achieved by applying (100–900)-MHz sinusoidal signals to an external wire loop placed less than 5 mm over the sample and soldered onto an input port of the PCB. Relaxation oscillations are measured using a two-point configuration and amplifying the rf voltage output of a bias tee.

To explain the observed dynamics, we consider a basic relaxation oscillation model from the perspective of a shunted nanowire. Figure 1(c) depicts its two time domains. After the nanowire first switches into the normal state, the bias current $i_{\rm bias}$ is diverted to the shunt with a time constant of $\tau_1 = L/(R_s + R_w)$, where L is the inductance, R_s is the shunt resistance, and R_w is the resistance of the nanowire represented by the hotspot-resistance. Once the current through the nanowire falls below the retrapping current I_r and allows the nanowire to return to the superconducting state, the bias current is diverted back from the shunt with a time constant $\tau_2 = L/R_s$ until the switching current $I_{\rm sw}$ is reached and the wire becomes normal again. Here, we use $I_{\rm sw}$ to describe the bias current at which the nanowire transitions into the resistive state. This is distinct from the critical current I_c, which is the theoretical fluctuation-free depairing current of the nanowire. As noted in Ref. [19], $I_{\rm sw} < I_c$ due to the influence of fluctuations present in experimental systems. Thus, the total period of a single relaxation oscillation may be approximated as

$$T = -\tau_1 \ln\left(\frac{I_r}{I_{\rm sw}}\right) - \tau_2 \ln\left(\frac{i_{\rm bias} - I_{\rm sw}}{i_{\rm bias} - I_r}\right). \qquad (1)$$

Since R_s tends to be much less than R_w, the duration set by τ_2 is expected to dominate the oscillation frequency, as is found in a similar modeling of relaxation oscillations in hysteretic Josephson bridge contacts [20].

III. RESULTS AND DISCUSSION

A. Characteristics of electrothermal relaxation oscillations

The expression given in Eq. (1) indicates that the frequency of the oscillation is a function of both the bias current and the inductance between the hotspot and the shunt resistor. Figure 2 shows our experimental data to investigate these dependences and compares the results with the simplified expression given in Eq. (1) and with electrothermal simulations conducted in SPICE [21,22]. The measurement is performed using a dc battery source in series with a 10-kΩ resistor to apply a steady current bias to the shunted device, and the oscillation frequency is extracted from the FFT of the amplified rf voltage output of the bias tee. The process is repeated for two different inductances in series with R_s, which is set by changing the distance between the shunt and the nanowire and, thus, altering the wire bond length. The hotspot-resistance R_w is used as a fitting parameter for both the electrothermal simulation and the relaxation oscillation model and is ultimately set equal to 500 Ω (corresponding to a length of about 500 nm over the 60-nm-wide region). For both models, the best-fit series inductance changes by roughly 25% between the two experiments with different wire bond lengths, revealing the significant impact of the path inductance on the nonlinear response of the shunted system. In addition to highlighting the influence of the series inductance on the overall dynamics of the shunted nanowire, the agreement between the experimental data and the two models indicates that the underlying mechanism of oscillation is indeed the electrothermal feedback between the hotspot and the shunt, rather than the nonlinearity of the superconducting current-phase relationship as in a Josephson junction.

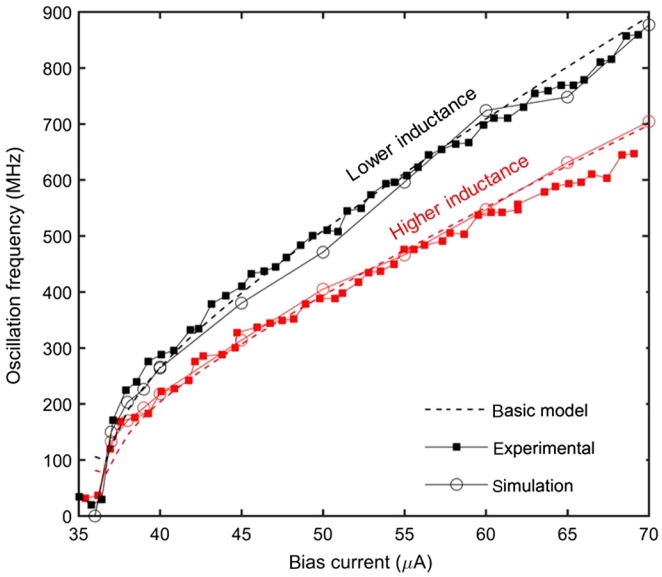

FIG. 2. Relationship between $i_{\rm bias}$ and the oscillation frequency for two different series inductances (red and black curves). The experimental data are compared to both electrothermal simulations and the basic relaxation oscillation model in Eq. (1). Parameters used to fit the red curve: $L = 20$ nH (basic model), $L = 25$ nH (simulation). Parameters used to fit the black curve: $L = 15.3$ nH (basic model), $L = 18.75$ nH (simulation). For all fits, $R_s = 10$ Ω and $R_w = 500$ Ω.

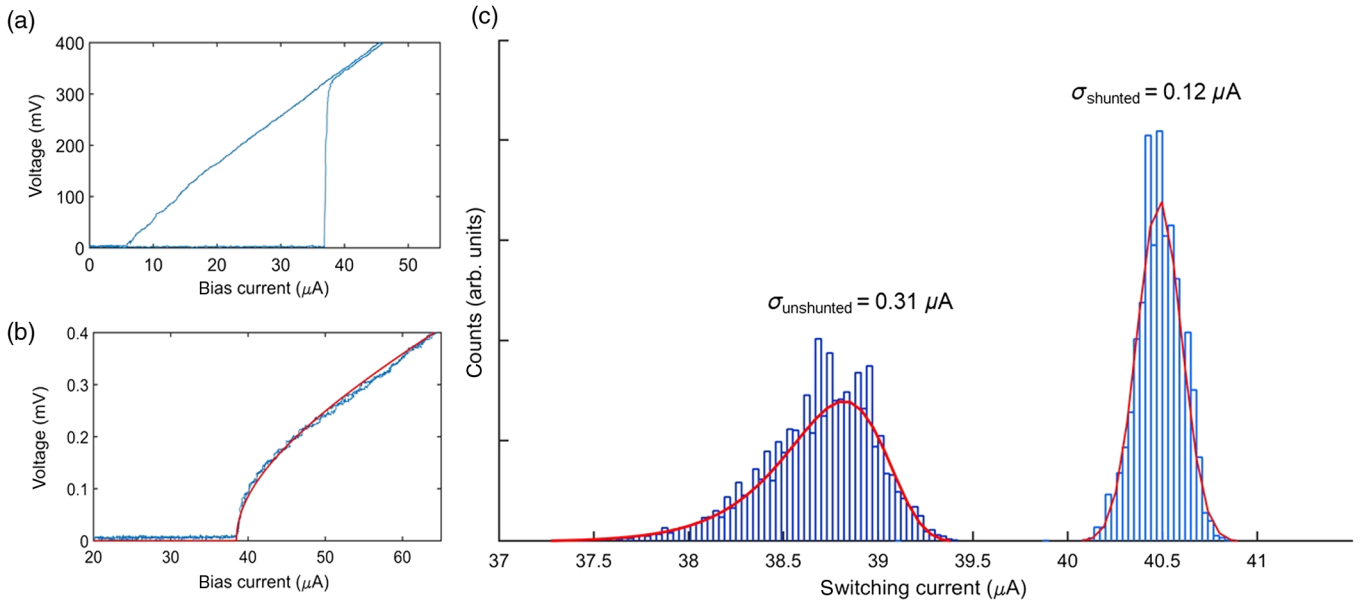

FIG. 3. (a) Current-voltage characteristics of the unshunted nanowire. (b) Current-voltage characteristics of the nanowire when it is shunted with $R_s = 10\ \Omega$. The red curve is a fit to an overdamped Josephson-junction model [Eq. (1)] with $I_c = 38.5\ \mu$A and $R = 7.8\ \Omega$. (c) Shunting the nanowire results in an increase in the mean and a narrowing in the width of the switching current distribution.

By reaching a maximum oscillation frequency close to the gigahertz range, such rapid oscillations can affect the shape of the current-voltage (I-V) characteristics conducted from a slow measurement, analogous to the key role played by fast Josephson oscillations in the I-V characteristic of a Josephson junction. In addition to impacting the frequency of these oscillations as described in Eq. (1), we observe that the shunt resistor significantly affects the amount of thermal dissipation in the nanowire, as indicated by the degree of hysteresis. Figures 3(a) and 3(b) show the I-V characteristics of the nanowire with and without the presence of an external shunt. Placing a resistance of 10 Ω in parallel with the wire results in complete suppression of hysteresis, suggesting a lack of sustained Joule heating [19,23]. The nonhysteretic I-V characteristic is fit to the expression for the average dc voltage of an overdamped Josephson junction in which the contribution of capacitance can be neglected [24],

$$V_{\mathrm{dc}} = I_c R \sqrt{(I_{\mathrm{bias}}/I_c)^2 - 1}, \tag{2}$$

where I_c is the critical current of the junction, R is the total parallel resistance, and I_{bias} is the current being supplied.

As illustrated in Fig. 3(b), we observe good qualitative agreement between the experiment and the overdamped junction model when the nanowire is shunted with 10 Ω and when the model resistance is set equal to 7.8 Ω. The slight discrepancy in resistance is not surprising, since the total parallel resistance $R = (1/R_{\mathrm{wire}} + 1/R_s)^{-1}$ is expected only to reach the full value of R_s when the self-heating hotspot-resistance has grown to the order of 1–10 kΩ. Such a large hotspot-impedance is avoided in a sufficiently shunted system if the resistance is low enough to divert the bias current after initial hotspot-formation, limiting the Joule-heated expansion of the normal domain. Other simplifications in the model including a lack of noise and capacitance terms may also contribute to this deviation. Nonetheless, the qualitative agreement suggests a relationship between the shunted nanowire and an overdamped Josephson-junction approximation, despite the presence of hotspots in the nanowire. Additionally, we observe that the shunt produced a narrowing in the width and an increase in the mean of the switching current distribution [Fig. 3(c)]. This observation has previously been explained in nanowires from the perspective of the Josephson-junction tilted-washboard-potential model as an increased damping which reduces the likelihood of the phase particle entering the running voltage state by a single thermal fluctuation [25]. As a result, the mean switching current increases, and the distribution becomes narrower due to the reduced impact of thermal fluctuations. While these changes show that resistive shunting limits the expansion of the hotspot, they also demonstrate that the absence of hysteresis and a narrowing of the switching distribution are not sufficient criteria for arguing that the nanowire is without Joule heating; rather, they indicate only that there is no sustained Joule heating on the time scale of the slow measurement.

B. Influence of microwave radiation

Although time-averaged I-V characteristics mask the direct observation of relaxation oscillations, they may provide evidence of oscillation locking under the influence of external modulation, as in the ac Josephson effect. To conduct this investigation, four-point electrical

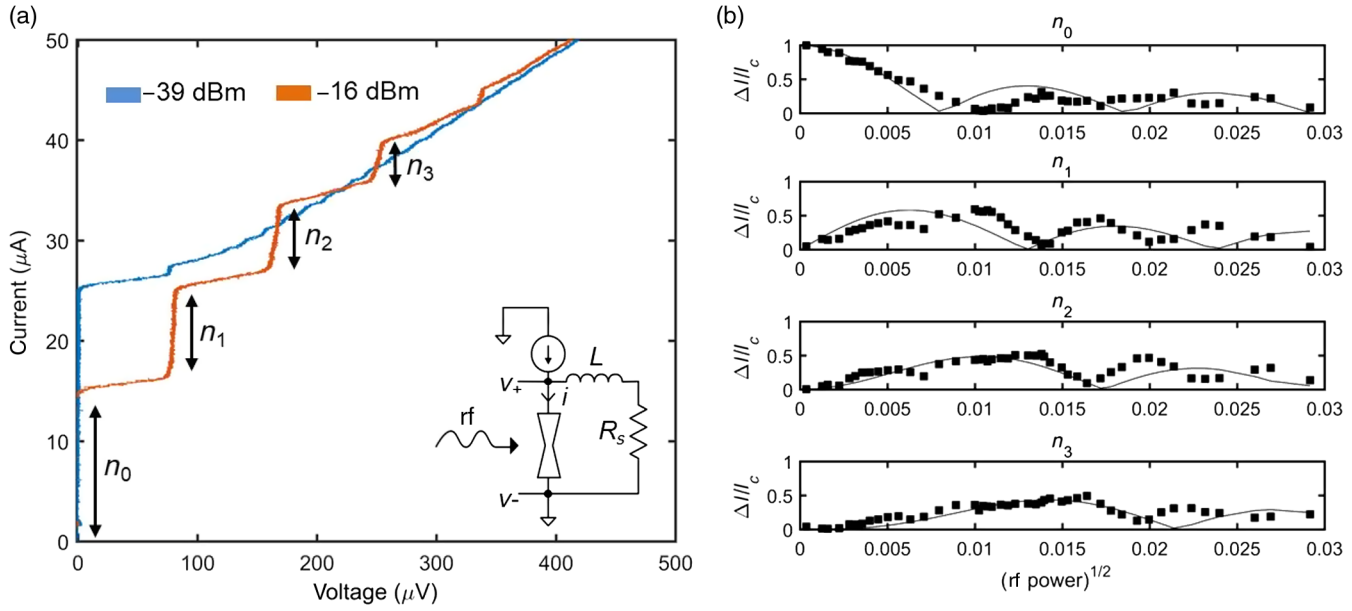

FIG. 4. (a) Steps appearing in the current-voltage characteristics with 180-MHz radiation at two different powers. (b) Amplitudes of the first four current steps as a function of the modulation power. Amplitudes are scaled relative to I_c, the magnitude of the n_0 step when no radiation is applied. The solid black curve shows fits to dynamical solutions for a Josephson junction following the expression $|J_n(2e\alpha V/hf)|$ as described in Ref. [26], where $\alpha = 1 \times 10^{-4}$.

characterization measurements are repeated while subjecting the shunted nanowire to external microwave radiation. As shown in Fig. 4(a), applying a 180-MHz sinusoidal drive to the coil antenna suppresses the nanowire's switching current and produces distinct steps in the I-V characteristics; the relative amplitudes of these steps appear to have a Bessel-like relationship with the microwave power, eventually decaying to zero when the switching current is fully suppressed and the nanowire enters the normal state [shown in Fig. 4(b)].

This phenomenon is similar to the Shapiro effect in Josephson junctions. Indeed, fits to the step amplitudes as a function of the modulation power can be made using Josephson-junction dynamical equations, as previously done for superconducting Dayem bridges [26]. In this case, step amplitudes follow the amplitudes of the nth-order Bessel functions $J_n(2e\alpha V/hf)$, where V is the magnitude of the external modulation, and α is a fitting parameter describing the coupling loss between the coil and the nanowire in order to convert from the known output power to the unknown voltage delivered to the nanowire.

Despite this similarity, the steps occur at voltage intervals roughly 200 times the expected Shapiro voltage for a 180-MHz drive, a disparity that was also noted but not fully explained in the work by Hadfield *et al.* [16]. Furthermore, the slope of the steps increases with step number, unlike in the ac Josephson effect. By conducting electrothermal simulations (see the Supplemental Material [27]) of shunted nanowires with varying inductances and microwave drives, we observe that the voltage steps occur at intervals of roughly $V_n = nfLI_c$, where f is the frequency of the modulation, L is the total series inductance, and n is the step number corresponding to the number of relaxation oscillations per period of the drive. Applying this formula to the parameters listed by Hadfield *et al.* correctly predicts the steps that they observed experimentally, where a nanowire with $L_k = 500$ nH and $I_c \approx 30$ μA produced steps at voltage intervals of roughly 200 μV when driven at 13.4 MHz. Whereas the Shapiro voltage relies on the flux unit of the superconducting magnetic flux quantum $(h/2e)$, the flux described by these voltage steps is dictated by the LI_c product. As a result, it is clear that this behavior does not stem from a Josephson-like current-phase relationship but rather phase locking of the relaxation oscillations.

Frequency mixing and pulling of inductively shunted tunnel junctions to a weak periodic drive have previously been explored as a means of phase locking; the strong broadband oscillations of inductively shunted Josephson junctions were seen to mix with an injected narrowband signal, eventually producing a frequency spectrum peak at the injection frequency when the modulation power was sufficiently increased [12]. Figure 5 summarizes our search for similar dynamics in the resistively shunted nanowire. This investigation is conducted by examining the frequency spectrum of the rf voltage output at a steady bias current while subjecting the nanowire to increasing powers of microwave radiation. In addition to peaks appearing at the relaxation oscillation frequency $f_r = 504$ MHz and the drive frequency $f_d = 320$ MHz, peaks are also observed at mixing products $f_r \pm m(f_d - nf_r)$, where m and n are positive integers. For instance, a peak at 690 MHz represents the mixing product of $n = 1$ and $m = 1$, or $2f_r - f_d$. Furthermore, as the magnitude of the driving signal

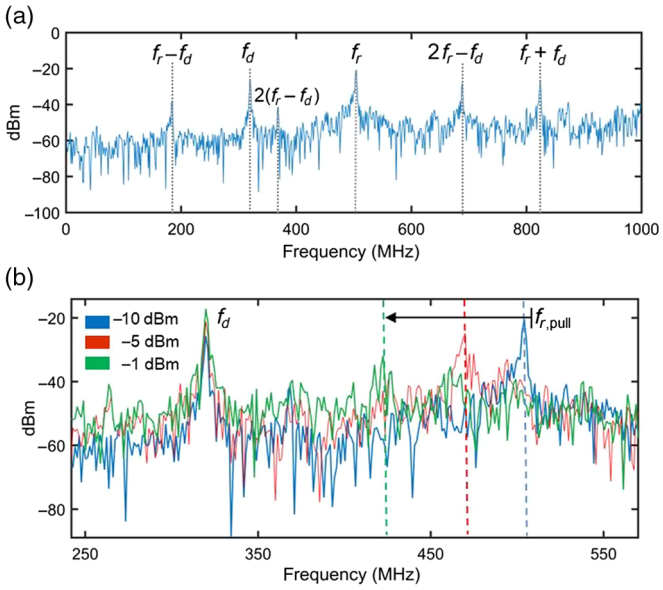

FIG. 5. (a) FFT of the voltage output with an applied radiation of 320 MHz and a constant bias current of 60 μA. Peaks indicate the resonance of the relaxation oscillations and the driving frequency, as well as their mixing products. (b) Enlarged view of the frequency spectrum while varying the applied microwave power. As the power increases, the relaxation oscillation frequency is pulled toward the driving frequency.

increases, the relaxation oscillation peak is pulled toward the driving frequency, and the mixing products shift in relation to the new f_r. This phenomenon is also observed at a bias condition where f_r is less than f_d (194 vs 330 MHz), demonstrating that the oscillation frequency can be pulled in either direction. The frequency shifting indicates possible applications of these devices in frequency up- or down-conversion for microwave signals.

While the mechanism of nonlinearity in our nanowires is electrothermal rather than due to the Josephson effect, it is nonetheless clear that the oscillations created by the interaction of the hotspot with an external shunt exhibit behavior analogous to that observed in Josephson junctions. The generation of mixing products is also similar to the result achieved with hot electron bolometers, which rely on the interference of a weak signal with a local oscillator to create an intermediate frequency signal that drives a thermally induced resistance change in a superconducting nanobridge upon absorption [28,29]. By getting pulled toward the drive signal until eventually locking, we observe that relaxation oscillations in the shunted nanowire circuit produce time-averaged characteristics that resemble the ac Josephson effect (see Fig. 4) without requiring a sinusoidal current-phase relationship.

IV. CONCLUSIONS

In summary, we present a study of the nonlinear dynamics in shunted nanowires and investigate their interaction with periodic external signals. While the noncoherent relaxation oscillations we observe originate from electrothermal effects, we find that they are capable of displaying qualitatively similar time-averaged characteristics and microwave responses as are observed in Josephson tunnel junctions. This result is summarized in our work by two main experimental findings: (1) We show that the frequency of relaxation oscillations due to the occurrence and collapse of a hotspot are strongly dependent on the applied bias current. Although this behavior is fundamentally different from Josephson oscillations, it produces similar nonhysteretic current-voltage characteristics that can be fit to the model for an overdamped junction. (2) The microwave modulation of these oscillations reveals pulling and mixing of the oscillation frequency with the application of a weak external drive, producing steps in the I-V characteristic that mimic the ac Josephson effect without matching the expected Shapiro voltage. A dual to the Shapiro voltage for relaxation oscillations is presented, where the flux is defined by the LI_c product rather than the magnetic flux quantum $h/2e$.

Because of the phenomenological similarities observed between the hotspot-relaxation oscillation and the Josephson oscillation, we envision that we can use these effects to develop nanowire-based microwave devices in certain applications where Josephson oscillations are conventionally employed. While the hotspot-relaxation oscillation is incoherent and slower than the Josephson oscillation, shunted nanowires maintain advantages such as a smaller device area and reduced sensitivity to magnetic noise or vortex dynamics. They can also be used in CMOS-compatible circuits without introducing the complexities of a current-phase relationship [30], and they may also be used to access frequencies in the range of approximately 100–1000 MHz where a Josephson-junction-based circuit requires additional large inductances. Microwave nanowire devices can be built with these benefits in mind; for example, modulation of the relaxation oscillation frequency by external signals may facilitate frequency multiplexing, as has been explored in injection-locked laser diodes [31,32], while prior work on tunnel junctions and point-contact Josephson junctions suggests that relaxation oscillations may also be used in mixing and parametric amplification [12,33]. Further reducing the inductance may also suppress the hotspot more efficiently, potentially allowing the nanowire to operate using faster, coherent oscillations more similar to those of a Josephson junction. Future studies of the gain and speed of these systems are required to recognize the feasibility of such applications.

ACKNOWLEDGMENTS

The authors thank Di Zhu, Andrew Dane, Brenden Butters, Marco Colangelo, Cyprian Lewandowski, Professor Leonid Levitov, and Professor Daniel Santavicca for scientific discussions, and Dr. Reza Baghdadi for scientific discussion and

proofreading of the manuscript. We also thank James Daley and Mark Mondol of the MIT Nanostructures Laboratory for technical support. This research is based on work supported by the Intel Corporation and by the Office of the Director of National Intelligence (ODNI), Intelligence Advanced Research Projects Activity (IARPA), via Contract No. W911NF-14-C0089. The views and conclusions contained herein are those of the authors and should not be interpreted as necessarily representing the official policies or endorsements, either expressed or implied, of the ODNI, IARPA, or the U.S. Government. The U.S. Government is authorized to reproduce and distribute reprints for governmental purposes notwithstanding any copyright annotation thereon. E. T. is supported by the National Science Foundation Graduate Research Fellowship Program under Grant No. 1122374.

E. T. fabricated the nanowires, A. M. supported the superconducting films and fabricated the gold contact pads, E. T. and Q.-Y. Z. took the measurements, E. T. analyzed the data and wrote the paper with input from K. B., Q.-Y. Z., and A. M., and K. B. supervised the project.

[1] B. van der, P. D. Sc, and J. van der Mark, LXXII. The heartbeat considered as a relaxation oscillation, and an electrical model of the heart, Lond. Edinb. Dublin Philos. Mag. J. Sci. **6**, 763 (1928).

[2] R. Lang and K. Kobayashi, Suppression of the relaxation oscillation in the modulated output of semiconductor lasers, IEEE J. Quantum Electron. **12**, 194 (1976).

[3] B. van der Pol and J. van der Mark, Frequency demultiplication, Nature (London) **120**, 363 (1927).

[4] B. D. Josephson, Possible new effects in superconductive tunnelling, Phys. Lett. **1**, 251 (1962).

[5] S. Shapiro, A. R. Janus, and S. Holly, Effect of microwaves on Josephson currents in superconducting tunneling, Rev. Mod. Phys. **36**, 223 (1964).

[6] M. T. Levinsen, R. Y. Chiao, M. J. Feldman, and B. A. Tucker, An inverse ac Josephson effect voltage standard, Appl. Phys. Lett. **31**, 776 (1977).

[7] R. L. Kautz, On a proposed Josephson-effect voltage standard at zero current bias, Appl. Phys. Lett. **36**, 386 (1980).

[8] O. A. Mukhanov, D. Gupta, A. M. Kadin, and V. K. Semenov, Superconductor analog-to-digital converters, Proc. IEEE **92**, 1564 (2004).

[9] P. W. Anderson and A. H. Dayem, Radio-Frequency Effects in Superconducting Thin Film Bridges, Phys. Rev. Lett. **13**, 195 (1964).

[10] K. K. Likharev, Superconducting weak links, Rev. Mod. Phys. **51**, 101 (1979).

[11] A. G. P. Troeman, S. H. W. van der Ploeg, E. Il'Ichev, H.-G. Meyer, A. A. Golubov, M. Y. Kupriyanov, and H. Hilgenkamp, Temperature dependence measurements of the supercurrent-phase relationship in niobium nanobridges, Phys. Rev. B **77**, 024509 (2008).

[12] N. Calander, T. Claeson, and S. Rudner, Relaxation oscillations in inductively shunted Josephson tunnel junctions, Phys. Scr. **25**, 837 (1982).

[13] A. J. Kerman, J. K. W. Yang, R. J. Molnar, E. A. Dauler, and K. K. Berggren, Electrothermal feedback in superconducting nanowire single-photon detectors, Phys. Rev. B **79**, 100509 (2009).

[14] A. J. Kerman, D. Rosenberg, R. J. Molnar, and E. A. Dauler, Readout of superconducting nanowire single-photon detectors at high count rates, J. Appl. Phys. **113**, 144511 (2013).

[15] D. K. Liu, L. X. You, S. J. Chen, X. Y. Yang, Z. Wang, Y. L. Wang, X. M. Xie, and M. H. Jiang, Electrical characteristics of superconducting nanowire single photon detector, IEEE Trans. Appl. Supercond. **23**, 2200804 (2013).

[16] R. H. Hadfield, A. J. Miller, S. W. Nam, R. L. Kautz, and R. E. Schwall, Low-frequency phase locking in high-inductance superconducting nanowires, Appl. Phys. Lett. **87**, 203505 (2005).

[17] A. E. Dane, A. N. McCaughan, D. Zhu, Q. Zhao, C.-S. Kim, N. Calandri, A. Agarwal, F. Bellei, and K. K. Berggren, Bias sputtered NbN and superconducting nanowire devices, Appl. Phys. Lett. **111**, 122601 (2017).

[18] H. L. Hortensius, E. F. C. Driessen, T. M. Klapwijk, K. K. Berggren, and J. R. Clem, Critical-current reduction in thin superconducting wires due to current crowding, Appl. Phys. Lett. **100**, 182602 (2012).

[19] M. Tinkham, J. U. Free, C. N. Lau, and N. Markovic, Hysteretic *I-V* curves of superconducting nanowires, Phys. Rev. B **68**, 134515 (2003).

[20] M. Mück, H. Rogalla, and C. Heiden, Relaxation oscillators made of bridge-type Josephson contacts, Appl. Phys. A **46**, 97 (1988).

[21] J. K. W. Yang, A. J. Kerman, E. A. Dauler, V. Anant, K. M. Rosfjord, and K. K. Berggren, Modeling the electrical and thermal response of superconducting nanowire single-photon detectors, IEEE Trans. Appl. Supercond. **17**, 581 (2007).

[22] K. K. Berggren, Q.-Y. Zhao, N. S. Abebe, M. Chen, P. Ravindran, A. N. McCaughan, and J. A. Bardin, Superconducting nanowire can be modeled by using SPICE, Supercond. Sci. Technol. **31**, 055010 (2018).

[23] W. J. Skocpol, M. R. Beasley, and M. Tinkham, Self-heating hotspots in superconducting thin-film microbridges, J. Appl. Phys. **45**, 4054 (1974).

[24] T. P. Orlando and K. A. Delin, *Foundations of Applied Superconductivity* (Addison-Wesley, Reading, MA, 1991), p. 461.

[25] M. W. Brenner, D. Roy, N. Shah, and A. Bezryadin, Dynamics of superconducting nanowires shunted with an external resistor, Phys. Rev. B **85**, 224507 (2012).

[26] P. E. Gregers-Hansen, M. T. Levinsen, L. Pedersen, and C. J. Sjøstrøm, Variation with microwave power of the current steps of superconducting microbridges, Solid State Commun. **9**, 661 (1971).

[27] See Supplemental Material at http://link.aps.org/supplemental/10.1103/PhysRevApplied.9.064021 for details on the electrothermal simulations used to confirm the synchronization of relaxation oscillations to microwave drives.

[28] E. M. Gershenzon, G. Gol'tsman, I. G. Gogidze, Y. P. Gusev, A. I. Elant'ev, B. S. Karasik, and A. D. Semenov, Millimeter and submillimeter range mixer based on electronic heating of superconducting films in the resistive state, Sov. Phys. Supercond. **3**, 1583 (1990).

[29] S. Cherednichenko, P. Khosropanah, E. Kollberg, M. Kroug, and H. Merkel, Terahertz superconducting hot-electron bolometer mixers, Phys. C Supercond. **372–376**, 407 (2002).

[30] Q.-Y. Zhao, A. N. McCaughan, A. E. Dane, K. K. Berggren, and T. Ortlepp, A nanocryotron comparator can connect single-flux-quantum circuits to conventional electronics, Supercond. Sci. Technol. **30**, 044002 (2017).

[31] L. Goldberg, H. F. Taylor, and J. F. Weller, FM sideband injection locking of diode lasers, Electron. Lett. **18**, 1019 (1982).

[32] Sze-Chun Chan, Frequency division multiplexed radio-over-fiber transmission using an optically injected laser diode, Proc. SPIE Int. Soc. Opt. Eng. **6997**, 69971Y (2008).

[33] Y. Taur and P. L. Richards, Relaxation oscillations in point-contact Josephson junctions, J. Appl. Phys. **46**, 1793 (1975).